

Quality Measures for Curvilinear Finite Elements



A. Johnen, C. Geuzaine, T. Toulorge, and J.-F. Remacle

Abstract We present a method for computing robust shape quality measures defined for finite elements of any order and any type, including curved pyramids. The measures are heuristically defined as the minimum of the pointwise quality of curved elements. Three pointwise qualities are considered: the *ICN* that is related to the conditioning of the stiffness matrix for straight-sided simplicial elements, the *scaled Jacobian* that is defined for quadrangles and hexahedra, and a new shape quality that is defined for triangles and tetrahedra. Based on previous work presented by Johnen et al. (Journal of Computational Physics 233:359–372, 2013, [1]); Johnen and Geuzaine (Journal of Computational Physics 299:124–129, 2015, [2]), the computation of the minimum of the pointwise qualities is efficient. The key feature is to expand polynomial quantities into Bézier bases which allows to compute sharp bounds on the minimum of the pointwise quality measures.

1 Introduction

With recent developments in the field of high-order finite element methods [3], such as discontinuous Galerkin [4] or spectral [5, 6] methods, there is a renewed interest

A. Johnen (✉) · J.-F. Remacle
Institute of Mechanics, Materials and Civil Engineering (iMMC), Université catholique de Louvain, Avenue Georges Lemaitre 4, 1348 Louvain-la-Neuve, Belgium
e-mail: amaury.johnen@uclouvain.be

J.-F. Remacle
e-mail: jean-francois.remacle@uclouvain.be

C. Geuzaine
Department of Electrical Engineering and Computer Science, Université de Liège, Grande Traverse 10, 4000 Lige, Belgium
e-mail: cgeuzaine@uliege.be

T. Toulorge
Cenaero, Rue des Freres Wright 29, 6041 Gosselies, Belgium
e-mail: thomas.toulorge@cenaero.be

© Springer Nature Switzerland AG 2021
C. Hirsch et al. (eds.), *TILDA: Towards Industrial LES/DNS in Aeronautics*,
Notes on Numerical Fluid Mechanics and Multidisciplinary Design 148,
https://doi.org/10.1007/978-3-030-62048-6_6

for high-order (curved) mesh generation. The classical finite element method, a.k.a. the *h*-version, uses linear elements to discretize the geometry and the mesh is refined in order to increase the accuracy of the solution. It has been established that the *p*-version of the finite element, for which the order of the functions is increased in order to improve the accuracy, may provide better convergence [7]. Eventually, “super-convergence” can be obtained by a mix of the two approaches [8]. There has been a frenzy in the 1980s to develop such methods, but developers encountered several difficulties which hampered their momentum [9] and consequently most of the current industrial-grade and commercial finite element packages are still based on at most second-order meshes. One reason is that during the process of generating a high-order curvilinear mesh, invalid (tangled) elements are often created, and untangling those is not a trivial task. Recent methods have improved the robustness of the untangling procedure through optimization, albeit at a high computational cost [10]. For this reason, the tendency is to apply the technique only on small groups of elements in the neighborhood of the invalid elements to untangle. It is therefore crucial to be able to detect invalid and poor-quality curvilinear elements.

A finite element is defined by the position of its nodes through a mapping between a reference element and itself. Its validity can thus be assessed by verifying the positivity of the determinant of the Jacobian of this mapping. It was thought for years that the only way to determine with certainty the validity of non-trivial elements would be by computing the Jacobian determinant at an infinite number of points [11, 12]. Recent developments based on Bézier interpolation showed that it is nothing of the sort. A first step has been taken in [13] where it is shown that it is possible to compute bounds on the Jacobian determinant of second order tetrahedra; those bounds are however not sharp. References [1, 2] provided a complete solution by developing an adaptive technique for efficiently computing the minimum and the maximum of the Jacobian determinant of any type and any order of elements, up to any prescribed tolerance. This method subsequently allows to guarantee the validity of any element.

Validity is one aspect that influences the accuracy of solution. Another aspect is the quality of the finite elements. A distinction can be made between geometric quality measures and Jacobian-based quality measures. Geometric quality measures have been used since the very early days of finite element modeling and are constructed from geometric characteristics such as the area/volume of the element, the length of the edges or the radii of the inscribed and circumscribed circles/spheres [14, 15]. These geometric quality measures are however not easily generalizable to curved elements—see e.g. [13] for the extension to quadratic tetrahedra. Jacobian-based measures are a more natural fit, since the Jacobian matrix is defined for all orders and types of element. A framework that allows the construction, classification, and evaluation of such measures defined on linear elements has been proposed in [16, 17]. It is important to understand that Jacobian-based measures are essentially pointwise (within the element). For the linear triangles and tetrahedra, this is not a problem since the Jacobian matrix is constant. For other elements, an element-wise measure has to be extracted from the pointwise measure. In the two references above, it is proposed to compute the measure at the corners of linear quadrangles and hex-

hedra and to take the minimum or the harmonic or geometric average. Similarly, for quadratic triangles, the element-wise measure can be computed as the minimum, maximum or the p^{th} power-mean of the pointwise measure sampled at the six nodes of the elements, although it is shown that in some situations this constitutes a poor approximation of the true minimum, maximum or p^{th} power-mean [12].

Many authors that have proposed curvilinear mesh generation techniques have only considered the validity or the ratio between the minimum of the Jacobian determinant over the maximum of the Jacobian determinant¹ in order to validate their resulting curved meshes [10, 18–26]. However, the Jacobian determinant only give information on area/volume and cannot be used as a quality measure. The ratio between the minimum and the maximum is neither a quality measure as highly deformed elements can present a constant Jacobian determinant [10]. This motivates the definition of proper quality measures for curved high-order finite elements.

Recent works have focused on defining a quality measure for curved simplicial finite elements of any order [27, 28]. The general approach is to consider the inverse of a Jacobian-based quality measure as proposed in [16], which constitutes a pointwise distortion measure. The L^2 -norm is computed in order to have an element-wise measure and the quality of the element is defined as the inverse of this element-wise distortion. The chosen distortion is such that it goes to infinity for degenerate (invalid) elements which implies that the corresponding quality vanishes. However, since the distortion measure is not a polynomial (it is at best a rational function), no exact computation of the measure is proposed and degenerate elements cannot robustly be detected by this method. Although developed for simplicial elements, this technique can be extended to non-simplicial elements, as shown in [29].

In this article, we propose to extend the method that efficiently computes the extrema of the Jacobian determinant as proposed in [1, 2] to Jacobian-based quality measures. Instead of computing the element-wise quality measure by simply taking a norm, we aim at finding the actual bounds of the pointwise measure. Three measures are considered: the ICN measure that is related to the conditioning of the stiffness matrix, the scaled Jacobian that is well-known in the hexahedral mesh community and a new one that is related to the error on the gradient of the finite element solution. Note that the goal of this article is not to study the correlation of the proposed quality measures with the error of finite element solutions, as e.g.. [30, 31]. Such study would be the subject of future works.

The article is organized as follows. In Sect. 2, we begin by recalling the Jacobian matrix of the different mappings before presenting the shape quality measures considered in this article. In Sect. 3, we present the Bézier expansion, we recall the algorithm for computing bounds on the validity of the elements and we give some properties of Bézier expansions that are useful for computing bounds on the quality measures. In Sect. 4, we explain how to compute those bounds. Finally, results are presented in Sect. 5 and we conclude in Sect. 6.

¹Note that those authors call this measure the “scaled Jacobian” while we use this name to denote another measure largely used by the hexahedral mesh community.

2 Definition of Quality Measures for Curvilinear Finite Elements

2.1 Background

Let us consider a mesh of order n , which consists of a set of curved physical elements that can either be triangles and/or quadrangles if the mesh has 2 dimensions or tetrahedra, hexahedra, prisms and/or pyramids if the mesh has 3 dimensions. 3D meshes are always defined in a 3 dimensional space. However, 2D meshes can either live in the xy -plane or be embedded inside a 3D surface that is in general non-planar. Let d_m and d_s denote respectively the dimension of the mesh and the dimension of the physical space in which the mesh is embedded. Each physical element is defined geometrically through a set of points of the physical space, called nodes, $\mathbf{n}_k \in \mathbb{R}^{d_s}$, $k = 1, \dots, N$ and a set of Lagrange shape functions $L_k^n(\boldsymbol{\xi}) : \Omega_{\text{ref}} \subset \mathbb{R}^{d_m} \rightarrow \mathbb{R}$, $k = 1, \dots, N$. These functions are polynomial and allow to map a reference unit element, whose domain of definition is Ω_{ref} , onto the physical one (see Fig. 1):

$$\mathbf{x}(\boldsymbol{\xi}) = \sum_{k=1}^N L_k^n(\boldsymbol{\xi}) \mathbf{n}_k . \quad (1)$$

Among the considered elements, pyramids are quite particular. Those elements which consist of a quadrangular base and four triangular faces have 4 edges that are incident to the summit node and cannot be defined by a polynomial mapping. Many different solutions have been proposed in the literature and among them, we consider the definition proposed in [32] that has optimal error estimates in H^1 -norm. Instead of polynomials, the mapping is defined by rational functions. Nevertheless, it has been shown that computing bounds on the Jacobian determinant of pyramids using the technique described in [1] is done as if it was defined by polynomials [2]. For simplicity, we will consider that all the elements have polynomial shape functions.

The Jacobian matrix of the mapping between the reference and the physical element, denoted by \mathbf{J}_R , is in general not constant over the element: $\mathbf{J}_R : \Omega_{\text{ref}} \rightarrow \mathbb{R}^{d_s \times d_m} : \boldsymbol{\xi} \mapsto \mathbf{J}_R(\boldsymbol{\xi})$. It is by definition the matrix of the first-order partial derivatives, i.e. $(\mathbf{J}_R)_{ij} = \frac{\partial x_i}{\partial \xi_j}$, which are polynomial functions. \mathbf{J}_R contains all the information of the transformation of the reference element into the physical element and can naturally be used to construct quality measures. However, as explained in [16], it may be necessary to compare the physical element to an *ideal* element which defines the ideal shape. This ideal element is usually the equilateral triangle or the square for 2D elements. We note the Jacobian matrix of the mapping between the ideal and the physical element \mathbf{J}_I . This matrix can be computed by the product $\mathbf{J}_I = \mathbf{J}_R \mathbf{W}^{-1}$, where \mathbf{W} is of dimension $d_m \times d_m$ and is the Jacobian matrix between the reference and the ideal element. In this article, we assume that \mathbf{W} is a constant matrix, therefore that the mapping between the reference and the ideal element is affine. We thus only consider ideal elements that are linear, have planar faces and (when appropriate) have

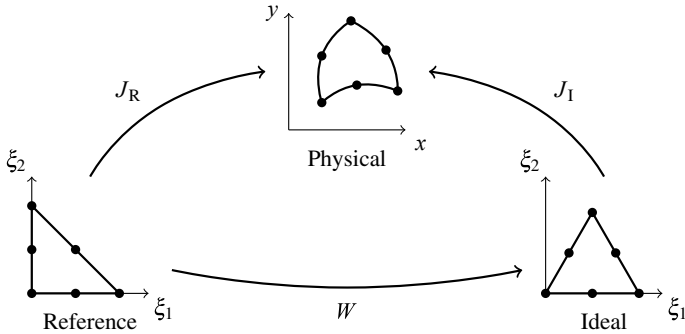


Fig. 1 We consider three mappings, each of them is characterized by a Jacobian matrix: (1) J_R for the mapping between the reference and the physical element, (2) W for the mapping between the reference element and the ideal element and (3) J_I for the mapping between the ideal and the physical element

parallel opposite sides. For instance, the ideal quadrangle can be a parallelogram but not a trapezoid. This implies that the elements of J_I remain polynomials, which is a necessary condition for computing the bounds the way it is presented in this article.

Finite element analyses are subject to discretization and roundoff errors that should be controlled. Those errors can be bounded by estimators that usually depend on the mesh through the size, shape, orientation of the elements, etc. [33]. The shape of the elements can also influence the speed of convergence of iterative methods. Quality measures allow to quantify those influences and to compare meshes. In the following, we define three pointwise shape quality measures. Some are orientation-sensitive, i.e. they take a negative value where the element is folded, and some are orientation-free. In this article, we consider only valid elements that pass the algorithm presented in [1] and for those elements, all the three measures take value between 0 and 1, with 1 being the quality of the perfect element. We also give a definition for the element-size measure at the end of this section.

2.2 The ICN Measure

Finite element formulations are solved using either iterative or direct methods. In iterative methods, it is highly desirable to minimize the condition number of the stiffness matrix as it influences the speed of convergence. In direct methods, a high condition number of the stiffness matrix rarely influence the computation time but still can introduce roundoff error [15].

The inverse of the condition number, up to a constant factor, constitutes a shape quality measure (see [16], Proposition 9.3). However, the condition number is hard to compute and an equivalent measure is preferred. Let us consider the following quantity defined on any given element E [16, 29, 34, 35]:

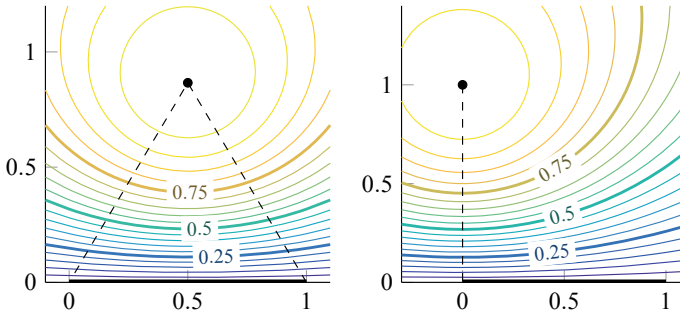


Fig. 2 The ICN measure for a straight-sided triangle when the *ideal* triangle is equilateral and the bottom left corner of a straight-sided quadrangle when the *ideal* quadrangle is squared

$$\eta_{pw}(E, \xi) = \frac{d_m |\mathbf{J}_1|^{\frac{2}{d_m}}}{\|\mathbf{J}_1\|_F^2} \quad \xi \in \Omega_{ref}, \tag{2}$$

where $|\cdot|$ stands for the determinant of a square matrix and $\|\cdot\|_F$ is the Frobenius norm of a matrix, i.e. $\|\cdot\|_F^2$ is the sum of the squares of the matrix elements. It follows from Proposition 8.7 of [16] that this quantity is equivalent to the inverse of the condition number. It subsequently measures the distance of \mathbf{J}_1 to the set of singular matrices (see Proposition 9.5 of the same paper). Thus, η_{pw} measures the pointwise distance to a locally degenerate element. We call this measure *ICN* as short for the inverse of the condition number. Figure 2 shows the contour plot of the ICN measure for a linear triangle and a linear quadrangle. The measure takes the maximum value of 1 when the element is locally of the same shape than the *ideal* element.

Note that a more accurate measure for the conditioning of stiffness matrices has been considered in [36] (see Sect. 3 and Appendix E). The algorithm to compute that measure is however very complex and leads to computation times that are about 10 times higher than the measure we consider in this article.

2.3 The New Shape Quality Measure for Triangles and Tetrahedra

In addition to the conditioning of the stiffness matrix, finite element analyses are also subject to discretization errors. We can consider essentially two discretization errors: the error on the solution and the error on the gradient of the solution. The former is only influenced by the size of the elements (and no shape quality can be derived). The latter is influenced by both the size and shape of the elements which harden the derivation of a *pure* shape quality measure. For straight-sided simplices, it is well-known that only large obtuse angles are bad for the error on the gradient [15]. The bound on the error on the gradient for a straight-sided triangle B depends on the

length of the three edges, l_{\min} , l_{med} and l_{\max} , the area A and the inscribed radius r_{in} :

$$B = c \frac{l_{\max} l_{\text{med}} (l_{\min} + 4r_{\text{in}})}{4A},$$

where c is a constant (see Table 2 of [15]). Figure 3a represents this bound on a contour plot. It goes to infinity for *caps* (triangles that have a large angle) but goes to $1.5c$ for *needles* (triangles that have a very small angle and the two other right). This means that needles are clearly acceptable for this error and corresponding shape quality measures should not go to zero for those shapes. A quality measure can be derived by inverting this bound and multiplying by a characteristic length. Such a quality measure has been proposed by Shewchuk by choosing as the characteristic length the square root of the triangle area (see Table 4 of [15]). This quality measure is however not a pure shape quality measure since it goes to zero for needles (see Fig. 3b). Actually, the choice of the square root of the triangle area as the characteristic length amounts to compare elements of same area. In this condition, going from the equilateral shape to a needle shape implies to increase some edge length up to the infinity. The measure then goes to zero because of the size and not the shape.

Another choice of characteristic length is $\sqrt{l_{\text{med}}l_{\max}}$ which gives the expecting behaviour as the measure goes to 0.83 for the needle (see Fig. 3c). Yet smooth quality measures are preferable in order to be able to optimize meshes, which motivates us to construct a new shape quality measure.

In 2D, let \mathbf{v}_1 and \mathbf{v}_2 be the two columns of the matrix \mathbf{J}_R and let us define another vector: $\mathbf{v}_3 := \mathbf{v}_2 - \mathbf{v}_1$. The three vectors \mathbf{v}_1 , \mathbf{v}_2 and \mathbf{v}_3 can be seen as the three edges of the local infinitesimal triangle. For a straight-sided triangles, the 2-norm of those vectors is equal to the length of the three edges. Moreover, the Jacobian determinant, $|\mathbf{J}_R|$, can be seen as 2 times the area of the local infinitesimal triangle (and is exactly 2 times the area of a straight-sided triangle). Let $\|\cdot\|$ designate the 2-norm of a vector, then the new shape quality measure for triangles is given by

$$\mu_{\text{pw}}^{2\text{D}}(E, \xi) = \frac{2}{3\sqrt{3}} \left(\frac{|\mathbf{J}_R|}{\|\mathbf{v}_1\| \|\mathbf{v}_2\|} + \frac{|\mathbf{J}_R|}{\|\mathbf{v}_1\| \|\mathbf{v}_3\|} + \frac{|\mathbf{J}_R|}{\|\mathbf{v}_2\| \|\mathbf{v}_3\|} \right),$$

where the terms of the sum are constructed by dividing the Jacobian determinant by the 2-norm of two vectors. Figure 3d shows the values that takes the new shape quality measure for a straight-sided triangle.

The new shape quality measure for tetrahedra is constructed similarly. Let \mathbf{v}_1 , \mathbf{v}_2 and \mathbf{v}_3 be the three columns of the matrix \mathbf{J}_R and let us define the vectors: $\mathbf{v}_4 := \mathbf{v}_2 - \mathbf{v}_1$, $\mathbf{v}_5 := \mathbf{v}_3 - \mathbf{v}_1$ and $\mathbf{v}_6 := \mathbf{v}_3 - \mathbf{v}_2$. Again, those vectors can be seen as the edges of the local infinitesimal tetrahedron while $|\mathbf{J}_R|$ can be seen as 6 times its volume. The new shape quality measure for tetrahedra can be constructed by summing terms that corresponds to the Jacobian determinant divided by the 2-norm of three vectors. Among the set of the 20 possible triplet of vector, triplets of vectors that are on a face cannot be used, as their product do not correspond to a volume. The four triplets of vectors that touch a same node are not used either which imply

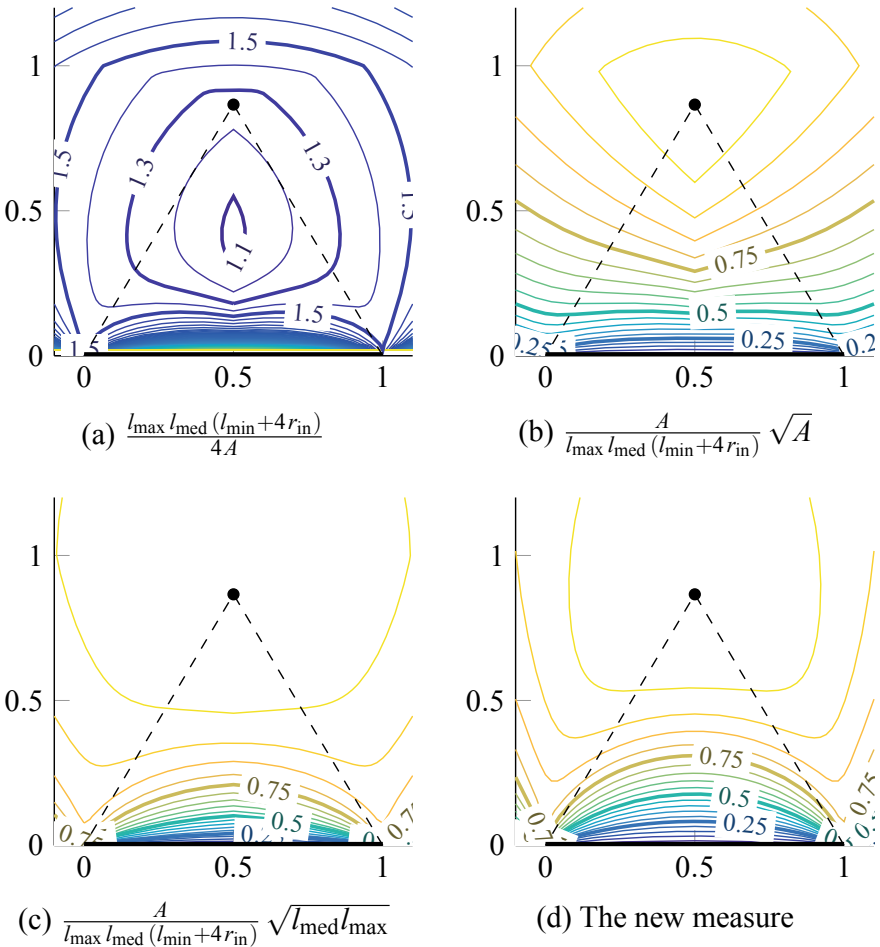


Fig. 3 **a** The bound of the error on the gradient for a straight-sided triangle and the corresponding quality measure obtained by inverting and multiplying by **b** \sqrt{A} and **c** $\sqrt{l_{\text{med}} l_{\max}}$. **d** The new shape quality measure for triangles. The three quality measures are normalized such that they are equal to 1 for the equilateral triangle

a set of 12 triplets:

$$\mathcal{J} = \{(1, 6, 2), (2, 5, 1), (3, 4, 1), (1, 6, 3), (2, 5, 3), (3, 4, 2), (1, 6, 4), (2, 5, 4), (3, 4, 5), (1, 6, 5), (2, 5, 6), (3, 4, 6)\} .$$

Then, the quality measure for tetrahedra is given by

$$\mu_{pw}^{3D}(E, \xi) = \frac{1}{\sqrt{2}} \left(\sum_{(i,j,k) \in S} \frac{|J_R|}{\|v_i\| \|v_j\| \|v_k\|} \right).$$



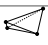

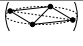


As usual, the quality of the equilateral triangle/tetrahedron is 1. In order to compare this new quality measure with the smooth quality measure proposed by Shewchuk, we look at the limit value of the two measures for the different shapes of the tetrahedron (see Table 1).

It is known that some shape are bad for the error on the gradient of the finite element solution and some other are good [15]. The new quality measure correctly takes that into account while it is not the case of the quality measure proposed by Shewchuk. We have to highlight that some authors have considered that shape quality measures must be zero for degenerate elements [16, 37] which is not the case of the new shape quality measure. We consider that the definition given by those authors is too restrictive as Shewchuk have shown in [15] that needles (which have a degenerate shape) are acceptable for the error on the gradient of finite element solutions.

2.4 The Scaled Jacobian Measure

The third quality measure we consider is the scaled Jacobian which is extensively used for measuring the quality of quadrangles and hexahedra [38–46]. It is defined as

Table 1 Limit values of the new quality measure compare to the one proposed by Shewchuk for bounding the error on the gradient of the finite element solution [15] for different shapes of the tetrahedron. The two quality measures are related to the error on the gradient of the finite element solution. But only the new one has a limit value different from zero for needles, flat wedges and long wedges, which are known to have only a slight impact on the gradient of the error. On the contrary, slivers, caps and spades can degrade the error on the gradient up to infinity

	Shape	μ_{pw}	Shewchuk [15]
Equilateral		1	1
Needle		0.61	0
Flat wedge		0.62	0
Long wedge		0.47	0
Sliver		0	0
Cap		0	0
Spade		0	0

$$\sigma_{pw}(E, \xi) = \frac{|J_R|}{\prod_j ||v_j||} .$$

Figure 4 represents this measure for a linear quadrangle. As the other measures, this measure takes its value between 0 and 1, with 1 being for the best shape and 0 for the worst.

2.5 Definition of an Element-Wise Measure

In order to define an element-wise measure for curved elements, we take the minimum of the pointwise measure:

$$\eta(E) = \min_{\xi \in \Omega_{ref}} \eta_{pw}(E, \xi) , \quad \sigma(E) = \min_{\xi \in \Omega_{ref}} \sigma_{pw}(E, \xi) ,$$

$$\mu(E) = \min_{\xi \in \Omega_{ref}} \mu_{pw}(E, \xi) .$$

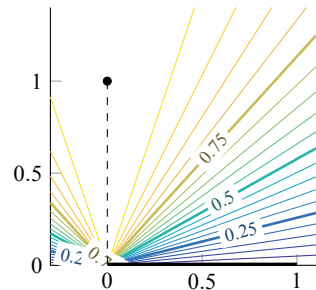
The rationale behind this is that it is certainly possible to bound the error of the finite element solution with this measure the same way we can bound the error by looking at the worst element of straight-sided meshes (and similarly for the condition number of the stiffness matrix).

3 Bézier Expansion: Definition and Properties

3.1 Definition

Polynomial quantities can be expanded into a so-called Bézier basis in order to make use of the well-known Bézier expansion properties. We introduce in this section all the concepts concerning the Bézier expansion that will be useful. Note that we use the multi-index notation for which $\mathbf{i} = (i_1, \dots, i_{d_m})$ is an ordered tuple of d_m indices.

Fig. 4 The Scaled Jacobian for the bottom left corner of a quadrangle



Let $B_i^v(\xi) : \Omega_{\text{ref}} \subset \mathbb{R}^{d_m} \rightarrow \mathbb{R}$, $i \in \mathcal{I}^v$ denotes a Bézier function of order v where \mathcal{I}^v is the index set of the Bézier functions. Both B_i^v and \mathcal{I}^v depend on the type of the element. The analytical expression of Bézier functions for linear, triangular, quadrangular, tetrahedral, hexahedral and prismatic elements are given in [1] and the expression for pyramidal elements is given in [2]. The set $\{B_i^v\}_{i \in \mathcal{I}^v}$ defines the *Bézier basis* of the polynomial space of order v . Let f_i denote the coefficients of the expansion, also known as the *control values*. For any polynomial function $f : \Omega_{\text{ref}} \subset \mathbb{R}^{d_m} \rightarrow \mathbb{R}$ of order at most v , one can compute the control values such that we have the equality

$$f(\xi) = \sum_{i \in \mathcal{I}^v} f_i B_i^v(\xi),$$

where the right member is the *Bézier expansion* of the function f .

The Bézier functions are positive and sum up to one which implies the well-known *convex hull* property. In our case, the convex hull property says that f is bounded by the extrema of the control values, i.e. $\min_i f_i \leq f(\xi) \leq \max_i f_i$. In addition to that, there are control values that are actual values of the expanded function. Those control values are “located” on the corners of the element² and we refer to their index set by \mathcal{I}_c^v . As a consequence, the control values allow to bound the two extrema of the function from below and above. For example, for the minimum we have: $\min_i f_i \leq f_{\min} \leq \min_{i \in \mathcal{I}_c^v} f_i$.

3.2 Workflow

Those bounds, computed from the Bézier expansion, are not necessarily sharp. However, they can be sharpened by subdividing, i.e. by expanding the same function defined on a smaller domain, called a subdomain. The smaller the subdomain, the sharper the bounds. This subdivision can be implemented in a recursive and adaptive manner which makes the method very efficient [1]. The algorithm for computing sharp bounds on polynomial functions consists of four steps:

1. Sampling of the function on a given set of points.
2. Transformation of those values into Bézier coefficients (by a matrix-vector product).
3. Computation of the bounds. If the sharpness is reached, return the bounds.
4. Subdivision (through a matrix-vector product). For each subdomain, go to step 3. Gather the “subbounds” and compute and return the global bounds.

We propose to adapt this algorithm to the computation of bounds of η_{pw} , σ_{pw} and μ_{pw} . As it will be seen in Sect. 4, only the third step has to be adapted.

²Let ξ_c be the reference coordinates of one of the corners of the element. For any Bézier basis, there exists an index j such that $B_j^v(\xi_c) = 1$ and $B_k^v(\xi_c) = 0$, $\forall k \in \mathcal{I}^v \setminus \{j\}$. We have thus the following equality: $f(\xi_c) = f_j$.

3.3 Properties

Additional properties of the Bézier expansion will be needed and are given in this section.

Proposition 1 Any Bézier function (even pyramidal) is of the canonical form $B_i^v(\xi) = \alpha_i^v m_i^v(\xi)$, where the coefficient α_i^v is a product of binomial coefficients and m_i^v is the elementary function.

As an example, let us consider the triangular Bézier functions³:

$$B_{i_1, i_2}^v(\xi, \eta) = \binom{v}{i_1} \binom{v-i_1}{i_2} \xi^{i_1} \eta^{i_2} (1-\xi-\eta)^{v-i_1-i_2} .$$

Its coefficient is $\alpha_{i_1, i_2}^v = \binom{v}{i_1} \binom{v-i_1}{i_2}$ and its elementary function is $m_{i_1, i_2}^v(\xi) = \xi^{i_1} \eta^{i_2} (1-\xi-\eta)^{v-i_1-i_2}$.

Proposition 2 The product of two elementary functions m_i^v and m_j^μ is an elementary function equal to $m_{i+j}^{v+\mu}$.

Example:

$$m_{i_1, i_2}^v m_{j_1, j_2}^\mu = \xi^{i_1+j_1} \eta^{i_2+j_2} (1-\xi-\eta)^{v+\mu-(i_1+j_1)-(i_2+j_2)} = m_{i_1+j_1, i_2+j_2}^{v+\mu} .$$

Corollary 1 The product of two Bézier functions of order v and μ is a Bézier function of order $v + \mu$ with an adjustment coefficient:

$$B_i^v B_j^\mu = \frac{\alpha_i^v \alpha_j^\mu}{\alpha_{i+j}^{v+\mu}} B_{i+j}^{v+\mu} .$$

Proposition 3 Let f and g be two polynomial functions of respective order v and μ and let $f_i, \mathbf{i} \in \mathcal{I}^v$ and $g_j, \mathbf{j} \in \mathcal{I}^\mu$ be their respective control values. The product of f and g is a polynomial function of order $v + \mu$ whose control values h_k are equal to

$$h_k = \sum_{\substack{\mathbf{i} \in \mathcal{I}^v \\ \mathbf{j} \in \mathcal{I}^\mu \\ \mathbf{i} + \mathbf{j} = \mathbf{k}}} f_i g_j \frac{\alpha_i^v \alpha_j^\mu}{\alpha_k^{v+\mu}} , \quad \forall \mathbf{k} \in \mathcal{I}^{v+\mu} .$$

Proof Using the definition of the Bézier expansion and Corollary 1, we have the equalities

³Note that in the case of a 2D elements, the multi-index has 2 indices which explains that $\mathbf{i} = (i_1, i_2)$.

$$h = fg = \sum_{\substack{i \in \mathcal{I}^v \\ j \in \mathcal{I}^\mu}} f_i g_j \frac{\alpha_i^v \alpha_j^\mu}{\alpha_{i+j}^{v+\mu}} B_{i+j}^{v+\mu} = \sum_{k \in \mathcal{I}^{v+\mu}} \sum_{\substack{i \in \mathcal{I}^v \\ j \in \mathcal{I}^\mu \\ i+j=k}} f_i g_j \frac{\alpha_i^v \alpha_j^\mu}{\alpha_k^{v+\mu}} B_k^{v+\mu} .$$

Proposition 4 *Relaxation:* Let f and g be two polynomial functions of order v and let f_i and g_i , $\mathbf{i} \in \mathcal{I}^v$ be their respective control values. In order that $f(\boldsymbol{\xi}) \leq g(\boldsymbol{\xi})$, $\forall \boldsymbol{\xi} \in \Omega_{ref}$, it is sufficient that $f_i \leq g_i$, $\forall \mathbf{i} \in \mathcal{I}^v$.

Proof Since every Bézier function is positive on the reference domain,

$$f_i \leq g_i \Rightarrow f_i B_i^v(\boldsymbol{\xi}) \leq g_i B_i^v(\boldsymbol{\xi}) \quad \forall \boldsymbol{\xi} \in \Omega_{ref}, \forall \mathbf{i} \in \mathcal{I}^v .$$

The last proposition can be used to compute bounds on more complex functions. The following sections explain how to do it for rational functions and functions that are similar to a quadratic mean, i.e. that are written $\sqrt{f_1^2 + f_2^2 + \dots}$ where the f_k are polynomial functions.

3.4 Computing Bounds on Rational Functions

It is possible to compute bounds on rational functions whose denominator is known to be strictly positive or strictly negative. There are four cases depending on the sign of the denominator and on the specification of the required bound (lower or upper bound). In the following, we detail the method for computing a lower bound in the case of a strictly positive denominator. The adaptation for other cases is straightforward.

Let $\frac{f}{g}$ ($g > 0$) be the rational function, with f and g two polynomial functions and let r_m denote the lower bound of this rational function we want to compute. Since g is strictly positive, the lower bound has to satisfy $r_m g \leq f$. Let f_i and g_i , $\mathbf{i} \in \mathcal{I}^v$ be the control values of their respective Bézier expansion. Taking advantage of the *relaxation* (Proposition 4), we can solve the problem

$$\begin{aligned} & \max r_m \\ & \text{s.t. } r_m g_i \leq f_i \quad \forall \mathbf{i} \in \mathcal{I}^v . \end{aligned}$$

Note that the coefficients g_i can take a negative value even if g is strictly positive. This is an optimization problem with only one variable whose solution is straightforward. The inequalities represent upper or lower bounds for r_m in function of the sign of g_i . Two situations may occur. The global lower bound can be larger than the global upper bound, in which case the problem has no feasible solution. In the other case, if the global lower bound is smaller than the global upper bound, the solution is r_m equal

to the upper bound. Special cases happen when $g_i = 0$. On the one hand, if $f_i \geq 0$, the corresponding inequality is satisfied whatever the value of r_m . On the other hand, if $f_i < 0$, the corresponding inequality cannot be satisfied and the problem has no feasible solution.

3.5 Computing Bounds with Quadratic Mean-Like Functions

When a square root is present in an expression we want to bound, it may be possible to square the expression in order to obtain only polynomials. However, it is possible to construct a function that bounds from the above quadratic mean-like functions, as proved by the following proposition:

Proposition 5 *Let f and g be two polynomial functions of order v and let f_i and g_i be their control values. Let H be the function whose control values are $H_i = \sqrt{f_i^2 + g_i^2}$. Then, we have $\sqrt{f(\xi)^2 + g(\xi)^2} \leq H(\xi) \forall \xi$.*

Proof Since the two members of the inequality are positive, we can square the expression:

$$\begin{aligned} \sum_i f_i B_i^v(\xi)^2 + \left(\sum_i g_i B_i^v(\xi) \right)^2 &\leq \left(\sum_i \sqrt{f_i^2 + g_i^2} B_i^v(\xi) \right)^2 \\ \Leftrightarrow \sum_{i,j} (f_i f_j + g_i g_j) B_i^v(\xi) B_j^v(\xi) &\leq \sum_{i,j} \sqrt{f_i^2 f_j^2 + f_i^2 g_j^2 + g_i^2 f_j^2 + g_i^2 g_j^2} B_i^v(\xi) B_j^v(\xi) . \end{aligned}$$

By the relaxation of Proposition 4, it is sufficient to prove the inequalities

$$f_i f_j + g_i g_j \leq \sqrt{f_i^2 f_j^2 + f_i^2 g_j^2 + g_i^2 f_j^2 + g_i^2 g_j^2} \quad \forall i, j .$$

The right-hand member is positive which implies that it is sufficient to prove that the relation holds when the members are squared. We obtain

$$\begin{aligned} 2 f_i f_j g_i g_j &\leq f_i^2 g_j^2 + g_i^2 f_j^2 \quad \forall i, j \\ \Leftrightarrow 0 &\leq (f_i g_j - g_i f_j)^2 \quad \forall i, j , \end{aligned}$$

which is true. □

Note that this lemma can be generalized to any function of the form $\sqrt{f_1^2 + f_2^2 + f_3^2 + \dots}$ where the f_k are polynomial functions. This result is useful in order to avoid to compute more coefficients as it is shown in the following section.

4 Computing Bounds on the Quality Measures

The computation of bounds for the considered quality measures relies on the fact that steps 1, 2 and 4 of the algorithm described in Sect. 3 are valid for any polynomial function. We can thus identify polynomial components of a given measure and directly apply steps 1, 2 and 4 to those components. Only the computation of the bounds in replacement of the 3rd step has to be modified.

The three measures can be computed from the same polynomial components. Let \mathbf{J} denote the Jacobian matrix used in the measure (\mathbf{J}_I for the ICN and \mathbf{J}_R for the new measure and the scaled Jacobian). Let $a_{i,j}$, $i, j = 1, \dots, d_m$ denote the elements of \mathbf{J} . They are polynomial functions and can be expanded into the Bézier basis of the mapping (1), i.e. into $\{B_i^n\}_{i \in \mathcal{I}^n}$. It is possible to compute the Jacobian determinant, the Frobenius norm of \mathbf{J} and the 2-norm of the columns of \mathbf{J} (which are sufficient to compute the three measures) only from the Bézier coefficients of the $a_{i,j}$. However, computing the Jacobian determinant from the $a_{i,j}$ is costly and we prefer to directly expand $|\mathbf{J}|$. Contrary to [1, 2], the Bézier basis in which it is expanded cannot be reduced for certain types of elements, it has to be $\{B_i^{2n}\}_{i \in \mathcal{I}^{2n}}$ for 2D elements and $\{B_i^{3n}\}_{i \in \mathcal{I}^{3n}}$ for 3D elements.

4.1 The ICN Measure

In 2D, the ICN measure is $2|\mathbf{J}_I| / \|\mathbf{J}_I\|_F^2$, where $\|\mathbf{J}_I\|_F^2 = \sum_{i,j} a_{i,j}^2$. The Bézier coefficients of the numerator are available since it is the Jacobian determinant. The denominator is also a polynomial function and the lower bound of the measure can be computed by the rational function technique provided that the denominator is expanded into the same Bézier basis than the numerator (Sect. 3.4). To do so, the expansion of the terms $a_{i,j}^2$ is computed thanks to Proposition 3 and the Bézier coefficients are summed in order to get the Bézier coefficients of the denominator.

In 3D, the measure is $3|\mathbf{J}_I|^{\frac{2}{3}} / \|\mathbf{J}_I\|_F^2$. In order to have a polynomial function at the numerator, the expression can be raised to the power of $\frac{3}{2}$ while still allowing us to compute a bound. Indeed, since the exponentiation is a monotonic operation and the measure is positive, whatever the bound r of $\eta_{pw}^{3/2}$ we compute, we will have that $r^{\frac{2}{3}}$ is a bound of η_{pw} . The denominator of the new expression is:

$$\|\mathbf{J}_I\|_F^3 = \left(\sqrt{\sum_{i,j=1}^3 a_{i,j}^2} \right)^3.$$

Due to the presence of the square root and since we are interested by a lower bound of the measure, we compute an upper bounding function of $\|\mathbf{J}_I\|_F$ by the technique described in Sect. 3.5. Afterwards, we apply Proposition 3 in order to obtain an expansion of the denominator into the same Bézier basis than the numerator. The

rational function technique can then be applied in order to compute the lower bound of the measure.

Let us recall that in 2D and 3D, an upper bound of the minimum of the measure is computed from the “corner” coefficients as explained in Sect. 3.

4.2 The Scaled Jacobian

The technique for computing a lower bound of the scaled Jacobian for quadrangles or hexahedra is the same. As for the other measure, we have to expand the denominator into the same Bézier basis than the numerator. The terms of the denominator are $||\mathbf{v}_j|| = \sqrt{\sum_i a_{i,j}^2}$. Since we are interested by a lower bound of the measure, we compute upper bounding functions V_j of $||\mathbf{v}_j||$ by the technique described in Sect. 3.5. The expansion of the denominator is then obtained by applying Proposition 3 on $\prod_j V_j$. Finally, the rational function technique gives the lower bound.

4.3 The New Measure

Each term of the new measure is exactly like the scaled Jacobian. It is then possible to compute a lower bound for each term, which would require to compute the upper bounding functions V_j in order to replace the $||\mathbf{v}_j||$. The sum of those bounds would be a lower bound of the quality measure but it would not necessarily be sharp since each term can take its global minimum at different points of the reference domain.

Instead, we transform the quality measure into a single fraction. We have

$$\mu_{pw}^{2D}(E, \xi) \geq \frac{2}{3\sqrt{3}} \frac{|\mathbf{J}_R| (V_1 + V_2 + V_3)}{V_1 V_2 V_3},$$

$$\mu_{pw}^{3D}(E, \xi) \geq \frac{1}{\sqrt{2}} \frac{|\mathbf{J}_R| \left(\sum_{(i,j,k) \in S} V_i V_j V_k \right)}{V_1 V_2 V_3 V_4 V_5 V_6}.$$

As for the two other quality measures, the numerator and denominator have to be expanded into the same Bézier basis. Then, the lower bound of the quality measure is computed by the rational function technique.

5 Results

The algorithm described in this article is implemented in Gmsh [47] and can be tested through the plugin `AnalyseCurvedMesh`. We begin this section by testing two linear hexahedra. Then, we test an academic hexahedral mesh with high differences in aspect ratio. Finally, we test a realistic mesh composed of curved tetrahedra. All the tests has been conducted on a Macbook Pro Retina, Mid 2012 @ 2.3GHz.

5.1 Single Hexahedron Test

Let us consider the case of a single hexahedron for which the nodes location is given in Table 2 of reference [11]. This hexahedron has positive Jacobian determinant on all the edges but is invalid. Traditional methods would compute a non-zero quality. Our algorithm computes the correct value of $\eta = \sigma = 0$. Now let us consider a more interesting case of a twisted hexahedron whose nodes location is given in Fig. 5.

This hexahedron is valid and the measures computed at a tolerance of 10^{-7} are in the range $\sigma \in [0.6891687332, 0.6891687876]$ and $\eta \in [0.5799706988, 0.5799707886]$. The minimum of σ_{pw} at the corners of the element is 0.6963, which is an error of 0.0071, while the minimum η_{pw} at the corners of the element is 0.6832, i.e. a substantial error of 0.1032. In order to compare with the basic method which consists in sampling the pointwise measure at a large number of points, let us consider the nodes of an hexahedron of order p . We sample the measures at the location of those nodes and compute the absolute error. As shown in Fig. 6, the error decreases slowly. With $p = 20$, which corresponds to 9, 261 sampling points, the error is still 3.68×10^{-4} for the ICN measure and 2.27×10^{-5} for the scaled Jacobian.

Fig. 5 Twisted hex:
Location and ordering of the nodes. Note that the convention for node order the one used in the Gmsh software

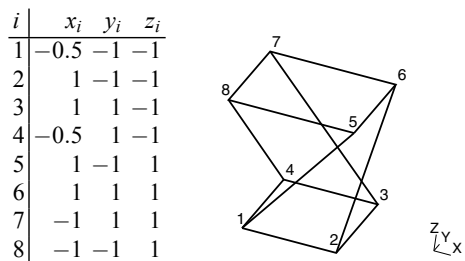
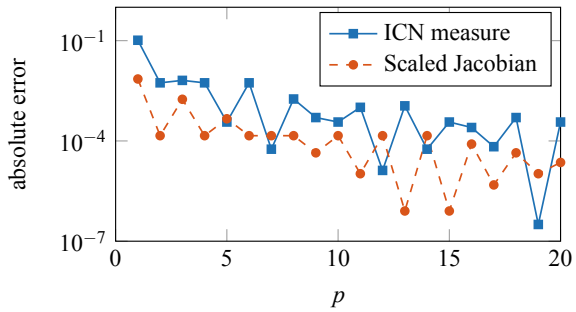


Fig. 6 Twisted hex:
 Absolute error of the sampling of η_{pw} and σ_{pw} at the nodes of an hexahedron of order p

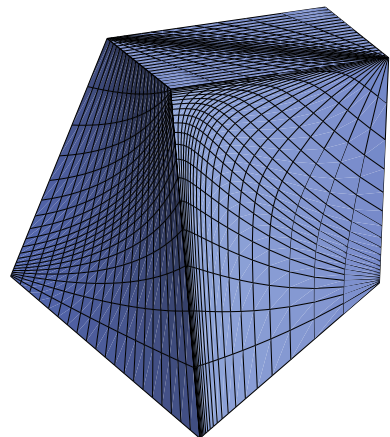


5.2 Academic Hexahedral Mesh

We now test the measures on a series of academic meshes composed of structured hexahedra. The meshes are generated with a mapping technique and presents high differences in sizes and aspect ratio, see Fig. 7. Three meshes are generated: a linear and a second-order mesh of 1,000,000 hexahedra and a third-order mesh of 125,000 hexahedra. For each mesh, the generation time and the time to compute the two measures are reported at Table 2. We also report in the same table the time to compute the validity of the different meshes, which corresponds to the time to compute the minimum and the maximum of the Jacobian determinant [1].

It is important to highlight that the mapping technique is characterized by a particularly fast execution time in comparison to the generation of other kind of meshes. Even though, the computation of one quality measure in those three tests is at most 29 times slower than the generation (for computing the scaled Jacobian on the third-order mesh). Compared to validity computation, the computation of one quality is at most 4.8 times slower (for computing the scaled Jacobian on the second-order mesh).

Fig. 7 Hex mesh: Coarse version (with 8,000 hexahedra) of the academic 1,000,000 and 125,000 hexahedra test cases



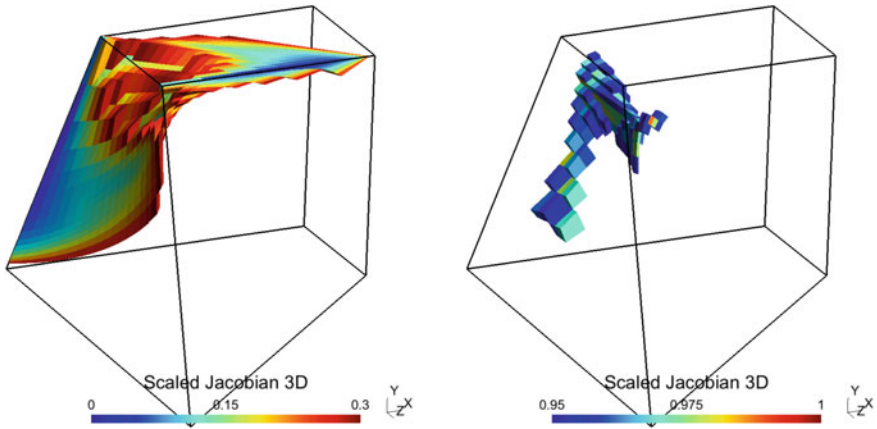


Fig. 8 Hex mesh: Worst (left) and best (right) quality elements of the coarse mesh

The worst and best elements according to the scaled Jacobian are shown in Fig. 8. As expected, the best elements have nearly the shape of a rectangular parallelepiped while the worst have large angles.

5.3 Realistic Curved Tetrahedral Mesh

Finally, we experiment the ICN measure (with the equilateral tetrahedron as the *ideal* element) and the new shape quality measure on a more realistic geometry that is

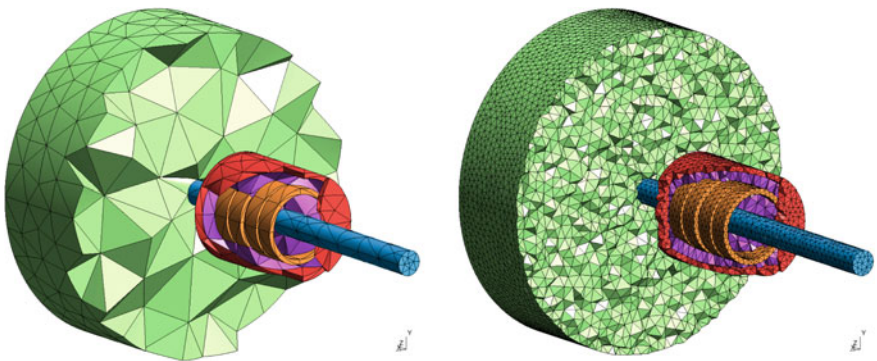


Fig. 9 Curved tetrahedral mesh: The geometry models a sensor for a steel cable. The geometry is composed of 4 coils (in orange), the cable (in blue) and the mounting box (in red). In purple and in green are respectively the interior and the exterior meshes of the voids. Left: coarse mesh. Right: fine mesh

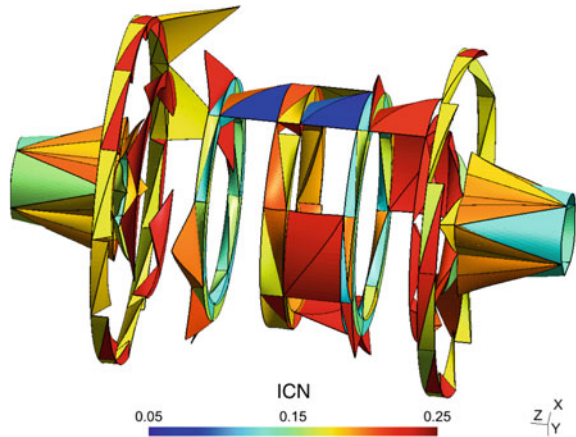
Table 2 Computation times of each test performed on the hexahedral and the tetrahedral mesh. Times are given in seconds. The generation time comprises the creation of 1D, 2D and 3D elements, the topological optimization of tetrahedral meshes (using Netgen [49]) and the geometrical optimization of high-order meshes (using [10]). $T(\eta)$, $T(\sigma)$ and $T(\mu)$ are the times to compute the measures described in this article while $T(\text{validity})$ is the time to compute [1]

Geometry	#elements	order	#vertices	T(gen.)	T(validity)	T(η)	T(σ)	T(μ)
Hexahedron	1,000,000	1	1,030,301	0.52	2.71	8.50	9.56	–
Hexahedron	1,000,000	2	8,120,602	36.98	33.60	123.00	160.00	–
Hexahedron	125,000	3	3,442,944	14.54	92.21	315.00	419.00	–
Magnet	6,440	3	32,478	40.52	0.37	1.27	–	2.25
Magnet	6,440	4	74,539	920.17	3.12	11.65	–	27.66
Magnet	341,962	1	64,145	17.41	0.60	1.19	–	1.76
Magnet	341,962	2	484,469	29.14	0.91	1.89	–	3.79
Magnet	341,962	3	1,603,146	45.66	5.55	10.39	–	28.85

meshed with tetrahedra. A coarse and a fine mesh are generated and optimized using the method presented in [10], see Fig. 9. In order to evaluate the computational cost of the new shape quality measure on first-order (straight-sided) meshes, we compare its computation time on the non-curved fine mesh with the computation time of a well-known (and widely used) measure that is the ratio between the insphere radius and the circumsphere radius [48]. The computation of the new measure takes 0.24 s/million tets while the computation of the ratio takes 0.49 s/million tets. This is explained by the fact that only the volume and edge length is needed to compute the new measure on straight-sided elements while the face area is also necessary to compute the ratio.

The execution time for computing the quality measures for the curved meshes is presented in Table 2. Note that, proportionally to the number of elements, the geometrical optimization takes more times for the coarse mesh than for the fine mesh because of the elongated/flat elements in the mountain box that are hard to optimize. This explains the particularly long generation time for the coarse mesh of order 4. A similar tendency appears with the computation of the validity and the ICN measure which takes more time per element on the coarse mesh than on the fine mesh. This is the consequence of a greater proportion of straight-sided elements and the presence of curved elements that are less distorted in the fine mesh. On the average, the number of subdivisions per element needed to reach the desired tolerance is 0.0414 for the fine mesh of order 3 and 1.7888 for the coarse mesh of order 3. The maximum number of subdivision on an element is 5 for the fine and 19 coarse mesh of order 3. Contrary to the hexahedral mesh, the computation of the measures for this tetrahedral mesh is smaller than the generation time. The worst elements of the coarse mesh are shown in Fig. 10.

Fig. 10 Curved tetrahedral mesh: Worst elements of the coarse mesh according to the ICN measure for an equilateral tetrahedron as the *ideal* element. Those elements are as expected located inside the mounting box



6 Conclusion

A method for computing the minimum of pointwise shape quality measures defined for any order and any type of common finite elements (including pyramids) has been presented. Three measures has been considered. The first one, the ICN measure, gives the deviation of shape with respect to the *ideal* element, the distance of the element to degeneracy and is also related to the conditioning of the stiffness matrix. The second one, the scaled Jacobian, is defined for quadrangles and hexahedra and is already widely used in the quadrangular/hexahedral mesh community. The third one is a new shape quality measure that works for triangles and tetrahedra and that is related to the error on the gradient of the finite element solution. The computation is efficient and numerical experiments show that for realistic third-order tetrahedral meshes the computation time of the quality measure is of the same order as the mesh generation time.

The ICN measure works well for isotropic meshes provided that the *ideal* element used to define the mapping is isotropic. This measure can possibly be extended for anisotropic meshes if the *ideal* element is function of the local metric, similarly to what has been done in [50]. The scaled Jacobian can be used when curved high aspect ratio quadrangles and hexahedra are needed, as for example in boundary layer meshes with high curvature. Those shape quality measures could give a robust base for the optimization of curvilinear meshes [10, 50, 51].

As the proposed extension of quality measures defined for straight-sided element to curved elements is heuristic, a study to show the correlation with the error of finite element solutions is another possible future work.

Acknowledgements A. Johnen is mandated by the Belgian Fund for Scientific Research (F.R.S.-FNRS). This research project was funded in part by the Walloon Region under WIST 3 grant 1017074 (DOMHEX) and by TILDA project.

References

1. A. Johnen, J.-F. Remacle, C. Geuzaine, Geometrical validity of curvilinear finite elements. *J. Comput. Phys.* **233**, 359–372 (2013)
2. A. Johnen, C. Geuzaine, Geometrical validity of curvilinear pyramidal finite elements. *J. Comput. Phys.* **299**, 124–129 (2015)
3. Z.J. Wang, K. Fidkowski, R. Abgrall, F. Bassi, D. Caraeni, A. Cary, H. Deconinck, R. Hartmann, K. Hillewaert, H.T. Huynh, N. Kroll, G. May, P.-O. Persson, B. van Leer, V. Miguel, High-order CFD methods: current status and perspective. *Int. J. Numer. Methods Fluids* **72**(8), 811–845 (2013)
4. R.M. Kirby, S.J. Sherwin, B. Cockburn, To CG or to HDG: a comparative study. *J. Sci. Comput.* **51**(1), 183–212 (2012)
5. P.E.J. Vos, S.J. Sherwin, R.M. Kirby, From h to p efficiently: Implementing finite and spectral/hp element methods to achieve optimal performance for low- and high-order discretisations. *J. Comput. Phys.* **229**(13), 5161–5181 (2010)
6. G. Karniadakis, S. Sherwin, *Spectral/hp element methods for computational fluid dynamics* (Oxford University Press, 2013)
7. I. Babuška, B.A. Szabo, I.N. Katz, The p-version of the finite element method. *SIAM J. Numer. Anal.* **18**(3), 515–545 (1981)
8. I. Babuška, B.Q. Guo, The h-p version of the finite element method for domains with curved boundaries. *SIAM J. Numer. Anal.* **25**(4), 837–861 (1988)
9. R.H. MacNeal, *Finite Elements* (CRC Press, 1993)
10. T. Toulorge, C. Geuzaine, J.-F. Remacle, J. Lambrechts, Robust untangling of curvilinear meshes. *J. Comput. Phys.* **254**, 8–26 (2013)
11. P.M. Knupp, On the invertibility of the isoparametric map. *Comput. Methods Appl. Mech. Eng.* **78**(3), 313–329 (1990)
12. P. Knupp, Label-invariant mesh quality metrics. in *Proceedings of the 18th International Meshing Roundtable* (Springer, 2009), pp. 139–155
13. P.L. George, H. Borouchaki, Construction of tetrahedral meshes of degree two. *Int. J. Numer. Methods Eng.* **90**(9), 1156–1182 (2012)
14. D.A. Field, Qualitative measures for initial meshes. *Int. J. Numer. Methods Eng.* **47**(4), 887–906 (2000)
15. J. R. Shewchuk, What is a good linear finite element? interpolation, conditioning, anisotropy, and quality measures (preprint), preprint (2002)
16. P.M. Knupp, Algebraic mesh quality metrics. *SIAM J. Sci. Comput.* **23**(1), 193–218 (2001)
17. P.M. Knupp, Algebraic mesh quality metrics for unstructured initial meshes. *Finite Elem. Anal. Des.* **39**(3), 217–241 (2003)
18. S.J. Sherwin, J. Peiró, Mesh generation in curvilinear domains using high-order elements. *Int. J. Numer. Methods Eng.* **53**(1), 207–223 (2002)
19. X. Luo, M.S. Shephard, R.M. O’bara, R. Nastasia, M.W. Beall, Automatic p-version mesh generation for curved domains. *Eng. Comput.* **20**(3), 273–285 (2004)
20. P.-O. Persson, J. Peraire, Curved mesh generation and mesh refinement using Lagrangian solid mechanics. in *47th AIAA Aerospace Sciences Meeting* (2009)
21. Z.Q. Xie, R. Sevilla, O. Hassan, K. Morgan, The generation of arbitrary order curved meshes for 3D finite element analysis. *Comput. Mech.* **51**(3), 361–374 (2013)
22. R. Abgrall, C. Dobrzynski, A. Froehly, A method for computing curved meshes via the linear elasticity analogy, application to fluid dynamics problems. *Int. J. Numer. Methods Fluids* **76**(4), 246–266 (2014)
23. D. Moxey, M. Green, S. Sherwin, J. Peiró, An isoparametric approach to high-order curvilinear boundary-layer meshing. *Comput. Methods Appl. Mech. Eng.* **283**, 636–650 (2015)
24. M. Fortunato, P.-O. Persson, High-order unstructured curved mesh generation using the Winslow equations. *J. Comput. Phys.* **307**, 1–14 (2016)
25. T. Liu, L. Wang, S.L. Karman Jr, C.B. Hilbert, Automatic 2d high-order viscous mesh generation by spring-field and vector-adding. in *54th AIAA Aerospace Sciences Meeting* (2016)

26. W.L. Shoemake, *Linear elastic mesh deformation via localized orthotropic material properties optimized by the adjoint method*. Ph.D. thesis (Dean College, 2017)
27. X. Roca, A. Gargallo-Peiró, J. Sarrate, Defining quality measures for high-order planar triangles and curved mesh generation. in *Proceedings of the 20th International Meshing Roundtable* (Springer, Berlin, 2012), pp. 365–383
28. A. Gargallo-Peiró, X. Roca, J. Peraire, J. Sarrate, Distortion and quality measures for validating and generating high-order tetrahedral meshes. *Eng. Comput.* 1–15 (2014)
29. A. Gargallo Peiró, Validation and generation of curved meshes for high-order unstructured methods. Ph.D. thesis (Universitat Politècnica de Catalunya, 2014)
30. W. Lowrie, V. Lukin, U. Shumlak, A priori mesh quality metric error analysis applied to a high-order finite element method. *J. Comput. Phys.* **230**(14), 5564–5586 (2011)
31. S.P. Sastry, R.M. Kirby, On interpolation errors over quadratic nodal triangular finite elements, in *Proceedings of the 22nd International Meshing Roundtable* (Springer, Berlin, 2014), pp. 349–366
32. M. Bergot, G. Cohen, M. Duruflé, Higher-order finite elements for hybrid meshes using new nodal pyramidal elements. *J. Sci. Comput.* **42**(3), 345–381 (2010)
33. B.A. Szabo, I. Babuška, *Finite element analysis* (Wiley, New York, 1991)
34. A. Liu, B. Joe, On the shape of tetrahedra from bisection. *Math. Comput.* **63**(207), 141–154 (1994)
35. A. Liu, B. Joe, Relationship between tetrahedron shape measures. *BIT Numer. Math.* **34**(2), 268–287 (1994)
36. A. Johnen, Indirect quadrangular mesh generation and validation of curved finite elements, Ph.D. thesis (Université de Liège, 2016)
37. J. Dompierre, P. Labbé, F. Guibault, R. Camarero, Proposal of benchmarks for 3d unstructured tetrahedral mesh optimization, in *Proceedings of the 7th International Meshing Roundtable* (Citeseer, 1998)
38. P.M. Knupp, Achieving finite element mesh quality via optimization of the Jacobian matrix norm and associated quantities. part I—A framework for surface mesh optimization. *Int. J. Numer. Methods Eng.* **48**(3), 401–420 (2000)
39. P.M. Knupp, Achieving finite element mesh quality via optimization of the Jacobian matrix norm and associated quantities. part II—A framework for volume mesh optimization and the condition number of the jacobian matrix. *Int. J. Numer. Methods Eng.* **48**(8), 1165–1185 (2000)
40. S. Yamakawa, K. Shimada, Fully-automated hex-dominant mesh generation with directionality control via packing rectangular solid cells. *Int. J. Numer. Methods Eng.* **57**(15), 2099–2129 (2003)
41. Y. Zhang, C. Bajaj, Adaptive and quality quadrilateral/hexahedral meshing from volumetric data. *Comput. Methods Appl. Mech. Eng.* **195**(9), 942–960 (2006)
42. Y. Ito, A.M. Shih, B.K. Soni, Octree-based reasonable-quality hexahedral mesh generation using a new set of refinement templates. *Int. J. Numer. Methods Eng.* **77**(13), 1809–1833 (2009)
43. M.L. Staten, R.A. Kerr, S.J. Owen, T.D. Blacker, M. Stupazzini, K. Shimada, Unconstrained plastering–Hexahedral mesh generation via advancing-front geometry decomposition. *Int. J. Numer. Methods Eng.* **81**(2), 135–171 (2010)
44. N. Kowalski, F. Ledoux, P. Frey, Automatic domain partitioning for quadrilateral meshing with line constraints. *Eng. Comput.* 1–17 (2014)
45. J.H.-C. Lu, I. Song, W.R. Quadros, K. Shimada, Geometric reasoning in sketch-based volumetric decomposition framework for hexahedral meshing. *Eng. Comput.* **30**(2), 237–252 (2014)
46. T.C. Baudouin, J.-F. Remacle, E. Marchandise, F. Henrotte, C. Geuzaine, A frontal approach to hex-dominant mesh generation. *Adv. Model. Simul. Eng. Sci.* **1**(1), 1–30 (2014)
47. C. Geuzaine, J.-F. Remacle, Gmsh: A 3-D finite element mesh generator with built-in pre-and post-processing facilities. *Int. J. Numer. Methods Eng.* **79**(11), 1309–1331 (2009)
48. P.-L. George, H. Borouchaki, Delaunay triangulation and meshing: application to finite elements (Hermes, Paris, 1998)

49. J. Schöberl, Netgen an advancing front 2d/3d-mesh generator based on abstract rules. *Comput. Visual. Sci.* **1**(1), 41–52 (1997)
50. A. Gargallo-Peiró, X. Roca, J. Peraire, J. Sarrate, Optimization of a regularized distortion measure to generate curved high-order unstructured tetrahedral meshes. *Int. J. Numer. Methods Eng.*
51. E. Ruiz-Gironés, A. Gargallo-Peiró, J. Sarrate, X. Roca, An augmented lagrangian formulation to impose boundary conditions for distortion based mesh moving and curving. *Procedia Eng.* **203**, 362–374 (2017)